Ship-in-a-Bottle Preparation of Long Wavelength Molecular Antennae in Lanthanide Metal–Organic Frameworks for Biological Imaging

Patrick Muldoon, Guillaume Collet, Svetlana Eliseeva, Tian-Yi Luo, Stephane Petoud, Nathaniel Rosi

Ship-in-a-Bottle Preparation of Long Wavelength Molecular Antennae in Lanthanide Metal-Organic Frameworks for Biological Imaging

Patrick F. Muldoon,† Guillaume Collet,‡§ Svetlana V. Eliseeva,‡ Tian-Yi Luo,† Stéphane Petoud,*‡† and Nathaniel L. Rosi*†⊥

†Department of Chemistry, University of Pittsburgh, Pittsburgh, PA 15260

‡Centre de Biophysique Moléculaire, Centre National de la Recherche Scientifique, 45071 Orléans, France.

§Le Studium Loire Valley Institute for Advanced Studies, 1 Rue Dupanloup, 45000 Orléans, France.

⊥Department of Chemical and Petroleum Engineering, University of Pittsburgh, Pittsburgh, PA 15260

ABSTRACT: While metal-organic frameworks (MOFs) have been identified as promising materials for sensitizing near-infrared emitting lanthanide ions (Ln^{3+}) for biological imaging, long-wavelength excitation of such materials requires large, highly delocalized organic linkers or guest-chromophores. Incorporation of such species generally coincides with fewer Ln^{3+} emitters per unit volume. Herein, the excitation bands of ytterbium-based MOFs are extended to 800 nm via a postsynthetic coupling of acetylene units to form a high density of conjugated π-systems throughout MOF pores. The resulting long wavelength excitation/absorption bands are a synergistic property of the composite material as they are not observed in the individual organic components after disassociation of the MOFs, thus circumventing the need for large organic chromophores. We demonstrate that the long wavelength excitation and emission properties of these modified MOFs are maintained in the biological conditions of cell culture (aqueous environment, salts, heating), pointing toward their promising use for biological imaging applications.

INTRODUCTION

The unique emissive properties of lanthanide ions (Ln^{3+}) combined with their natural abundance attract intense research interests in areas such as biological imaging, telecommunication devices, low cost lighting, energy conversion, and sensing.[1-2] Their strong resistance to photobleaching and sharp emission bands with characteristic wavelengths that are independent of experimental conditions make Ln^{3+} attractive candidates for detection in complex media such as biological systems. Near-infrared (NIR)-emitting Ln^{3+} (Nd^{3+}, Ho^{3+}, Er^{3+}, Yb^{3+}) are especially well-positioned for bioimaging applications because of the NIR transparency window of biological tissue[3], as well as for telecommunication devices and lasers. However, free Ln^{3+} suffer from the inefficiency of direct excitation of most transitions (absorptivities often below 1 $M^{-1}cm^{-1}$)[1, 4] and a high susceptibility to quenching due to the overtones of high energy vibrations from O-H, N-H and C-H bonds.[4-6] Emissive Ln^{3+}-based materials must therefore be designed to protect the Ln^{3+} from quenching and to incorporate chromophores that sensitize the Ln^{3+} through a process that is known as the "antenna effect".[6-7] The optimal excitation wavelength of the antennae depends largely on targeted applications. For example, some applications may require broadband excitation throughout the visible spectrum while others may require lower energy visible-NIR excitation. Therefore, an ideal matrix material for preparing Ln^{3+}-based emitters would i) contain a high density of both luminescent Ln^{3+} and sensitizing chromophores, ii) provide a sufficient level of protection of Ln^{3+} from sources of non-radiative deactivation, and iii) be amenable to structural and functional modification as a means to finely tune their luminescence properties.

Metal-organic frameworks (MOFs) allow an elevated level of organization of a high density of luminescent Ln^{3+} in well-defined coordination environments and provide means of photosensitization through chromophoric organic linkers or guest species.[8-19] However, for applications that make use of Ln^{3+} NIR emission such as optical bioimaging, long wavelength photosensitization is advantageous due to the minimization of the interaction between excitation light and the biological sample. This requirement implies that the corresponding organic molecular sensitizers be large, highly delocalized species.[20] Incorporating such species into a MOF requires large pore volumes or the use of long delocalized linkers. Both scenarios result in highly open frameworks with a lower density of Ln^{3+} emitters per unit volume and a corresponding decrease in emission intensities and detection sensitivities. In addition, the use of MOFs with highly spacious pores and/or longer, more exotic organic linkers can lead to lower stabilities and generally more demanding syntheses. An alternative strategy for achieving low energy sensitization of Ln^{3+}-based MOFs would be to prepare a high density of delocalized species in MOF nanopores by loading small molecular precursors into the MOFs which subsequently couple to form a dense array of π-systems. This "ship-in-a-bottle" synthetic approach in which the close-packing of π-systems induces longer wave-

length absorption as a supramolecular property would circumvent the need for large pores to accommodate large molecular dyes or large, highly delocalized organic linkers for MOF synthesis.

Here, two MOFs, **MOF-1114(Yb)** and **MOF-1140(Yb)**, consisting of 2-aminoterephthalate (NH_2-BDC) organic linkers and Yb^{3+}-based inorganic secondary building units (SBUs) with nanoscale porosity are postsynthetically modified[21] by coupling methyl propiolate (MP) with the linker-bound amine[22] to obtain a high density of short π-systems (2-4 conjugated π-bonds) confined in MOF pores. We demonstrate that the resulting modified MOFs exhibit longer wavelength absorption and photosensitization (up to 800 nm) of Yb^{3+} NIR emission (λ_{max}=980 nm). We also show that these observations result from a systemic property as they are not observed in the isolated modified organic linkers in solution or outside of the pores of the MOF. We identify the density of π-systems in these modified MOFs as a dominant factor for extending absorption and excitation cross sections to longer wavelengths. In respect to optical bioimaging applications, we demonstrate that the modified MOFs maintain their structure and emissive properties in the aqueous biological conditions of living cells. Collectively, these results represent major steps forward in creating MOF-based NIR imaging agents suitable for biological applications with tunable and optimized excitation wavelengths.

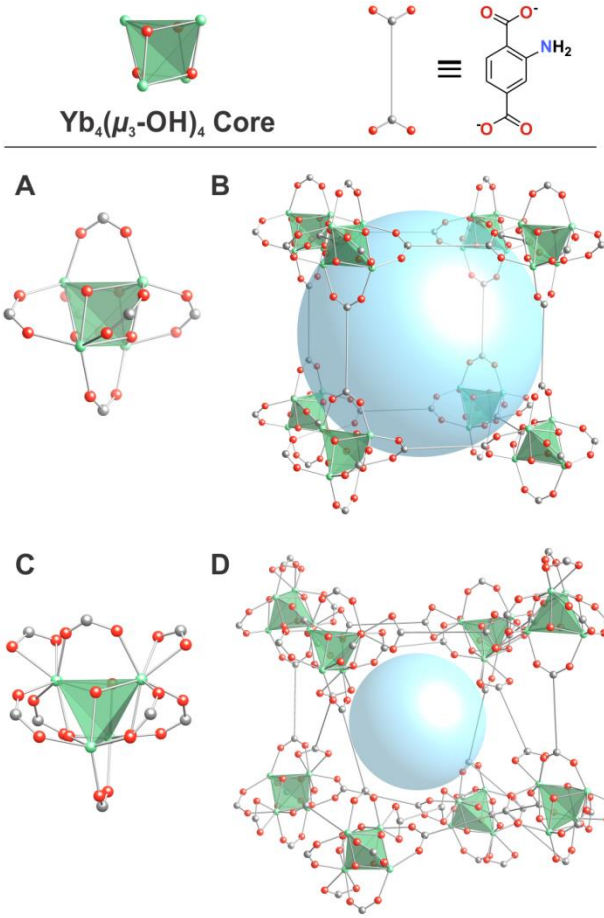

Figure 1. MOF structures (Yb^{3+}, green spheres; C, grey spheres; O, red spheres; green tetrahedron defines Yb^{3+} core; blue spheres represent pore volume; H atoms omitted for clarity). (A) Inorganic SBU of **MOF-1114(Yb)**; (B) Crystal structure of **MOF-1114(Yb)**; (C) Inorganic SBU of **MOF-1140(Yb)**; (D) Crystal structure of **MOF-1140(Yb)**.

RESULTS AND DISCUSSION

MOF-1114(Yb), $[Yb_4(\mu_3\text{-}OH)_4(NH_2\text{-}BDC)_3(H_2O)_8]\bullet 2Cl^-$, was synthesized following a protocol that we had developed previously (Supporting Information).[18] **MOF-1140(Yb)**, $Yb_4(\mu_3\text{-}OH)_4(NH_2\text{-}BDC)_{3.64}(CH_3CO_2)_{0.73}(H_2O)_6$, was synthesized by dissolving $Yb(CH_3CO_2)_3\bullet 4H_2O$ and H_2-NH_2-BDC in dimethylformamide (DMF) and heating at 100ºC for 70 hours. Both MOFs contain $[Yb_4(OH)_4]^{8+}$ clusters with four Yb^{3+} forming a tetrahedron with faces bridged by four μ_3-hydroxides (Figure 1). **MOF-1114(Yb)** exhibits **pcu** topology, where each edge-sharing Yb^{3+} pair is bridged by a carboxylate from an NH_2-BDC linker (Figure 1A and 1B). **MOF-1140(Yb)** likewise contains six Yb^{3+}-bridging carboxylates at each node as well as two additional non-bridging carboxylates, increasing the points of extension from 6 to 8 and decreasing the accessible pore volume (Figure 1C and 1D): Connolly free volumes were calculated from the crystal structures of **MOF-1114(Yb)** and **MOF-1140(Yb)** (sphere radius=0.75 Å) to be 68.5% and 54.0%, respectively.

MOF-1114(Yb) and **MOF-1140(Yb)** were reacted with MP to extend the π-systems of the linkers and to red-shift the absorption profile of the materials. MOF crystals were thoroughly washed with DMF followed by solvent exchange with acetonitrile (ACN). MOF crystals (~30 mg) along with 200 μL of ACN were then transferred to a vial containing 1.5 mL of MP. Four variants of this reaction were performed: crystals of either **MOF-1114(Yb)** or **MOF-1140(Yb)** were submerged in MP at room temperature or at 75ºC for ~24 hours, after which the product distribution as well as photophysical properties proved to be fully reproducible. A color change from colorless to red or orange was observed within a few hours (Figure 2). Crystals became visibly darker as the reaction proceeded over the course of 8 hours. After 24 hours, the crystals were washed with ACN to remove unreacted MP. Proton nuclear magnetic resonance (^{1}H NMR) spectroscopy and liquid chromatography mass spectrometry (LCMS) revealed that a mixture of four coupling products and unreacted H_2-NH_2-BDC were present after dissolution of MOFs in deuterated acidic solution (Figure 3A, S5-S13). Heating increased both the overall conversion of amines and the ratio of the larger diadducts (**d1** and **d2**) to monoadducts (**m1** and **m2**) in comparison to room temperature reactions (Figure 3B). In addition, the more porous and open **MOF-1114(Yb)** produced a higher overall conversion and a higher ratio of diadducts to monoadducts at a given temperature compared to **MOF-1140(Yb)**.

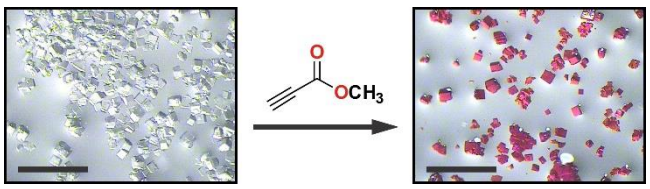

Figure 2. Brightfield optical microscopy images of **MOF-1114(Yb)** crystals before and after postsynthetic modification (PSM) with MP (scale bars=500 μm).

Solution absorption spectra of digested **MOF-1114(Yb)** and **MOF-1140(Yb)** (Figure 4A and 4B, black curves) show apparent λ_{max} around 365 nm that can be attributed to π-π* transitions of H_2-NH_2-BDC and the absence of significant absorption beyond 450 nm. After modification, solution absorption spectra of product mixtures, which we know from LCMS (Figure S5-S11) and ^{1}H NMR (Figure S13) analysis include unreacted H_2-NH_2-BDC, monoadducts, and diadducts, also show the absence of absorption beyond 450 nm (Figure 4A and 4B, red and blue curves). We can infer that the relatively sharp band centered at 315 nm that appears on the spectra of the product mixtures originates from the monoadduct isomers as it is not present in the solution-phase absorption spectra of pure **d1** or NH_2-BDC (Figure S14). Microspectrophotometry was used to measure the absorption spectra of intact MOF crystals before and after modification. We observed that the absorption spectrum of the H_2-NH_2-BDC in solution does not differ significantly from the one of the MOF in which it functions as a linker: the apparent absorption maximum shifts from 365 nm when recorded in solution to about 394 nm in the MOF structure, after which absorption decreases steeply (Figure 4A to 4D, black curves). The slight red-shift of linker-centered absorption is consistent with cases of comparable MOFs reported in the literature.[23] However, we observe a much stronger contrast between the solid-state absorption of the modified MOF crystals and the corresponding solution-phase product mixtures after dissolving the MOFs. We see that the absorption spectra of the modified MOFs are broad and extend toward lower energy up to 600 nm (Figure 4C and 4D, red curves). The fact that none of the organic components absorb beyond 450 nm in solution indicates that the long wavelength absorbance is a synergistic property of the composite material. Specifically, a dense amorphous packing of interdigitated π-bonds confined within relatively rigid MOF cavities results in a myriad of higher-order intermolecular orbital interactions.[24] This special organization would explain the long wavelength absorption as well as the relatively broad flat shape of the observed absorption bands.

A

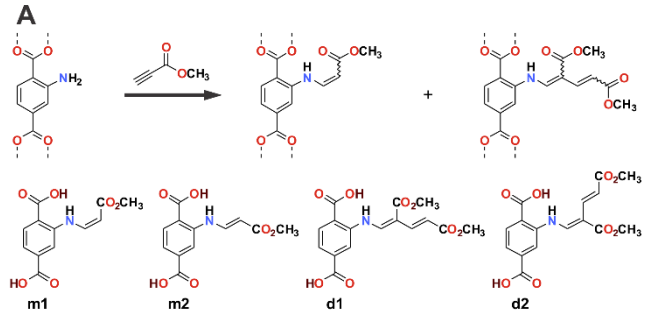

B

MOF	temp	NH_2-BDC %	m1 %	m2 %	d1 %	d2 %
MOF-1114(Yb)	r.t.	63	25	<1	12	<1
	75°C	39	9	<1	38	13
MOF-1140(Yb)	r.t.	81	11	4	4	<1
	75°C	64	10	<1	19	8

Figure 3. (A) Products of PSM reactions identified after the dissolution of MOFs as determined by ^{1}H NMR and LCMS; (B) Product ratios after the dissolution of modified MOFs as determined by ^{1}H NMR.

Emission spectra were collected on solid samples of **MOF-1114(Yb)** and **MOF-1140(Yb)** under DMF using a 380 nm excitation wavelength. These spectra reveal the characteristic Yb^{3+} emission signal with a sharp band possessing an apparent maximum around 980 nm which is assigned to the $^2F_{5/2}$-$^2F_{7/2}$ transition (Figure 4E and 4F). Each of these spectra reveal an additional shoulder on the low energy side of the 980 nm band of variable intensity most probably arising from the splitting of the fundamental emitting state due to ligand field effects.[25] As the Yb^{3+} cation does not possess excited states in the UV-visible energy domain, the sensitization of its characteristic emission upon 380 nm excitation unambiguously demonstrates the presence of an antenna effect provided by the MOF ligands.

Analysis of excitation spectra of **MOF-1114(Yb)** and **MOF-1140(Yb)** provides further insight into the different sensitization pathways in these systems. Excitation spectra were obtained by monitoring the emission intensity of Yb^{3+} in solid MOF crystals at 980 nm under DMF (Figure 4G and 4H, respectively). In both cases the excitation bands of the unmodified MOFs (black curves) can be attributed to sensitization by the electronic structure of NH_2-BDC as they extend up to 420-430 nm before declining sharply which matches well to corresponding absorption spectra (Figure 4C and 4D, black curves). Upon reaction with MP, these excitation bands are extended in the red/NIR range up to 700 nm (Figure 4G and 4H, blue and red curves) indicating that the modified MOF linkers are indeed functioning as longer wavelength antennae for Yb^{3+} emission. The capacity for modulating excitation wavelength is demonstrated by varying reaction temperature. Notably, the excitation spectra after r.t. modification (blue curves) extends to 700 nm while the modification at 75°C further extends the excitation wavelength up to 800 nm (red curves). Photosensitization of Yb^{3+} with excitation wavelengths above 700 nm is attractive for bioimaging applications as it places both emission and excitation wavelengths within the optical transparency window of biological tissue (650-1450 nm).[3] In all cases, the excitation bands contain multiple distinguishable components observed as local apparent maxima and shoulders on the excitation spectra. These features are attributed to the presence of various excited states located in the different chromophoric parts being monitored. In this case the source of light emission and light absorption are not unitary, so the shape of the excitation spectra will be affected not only by the electronic transitions located on the organic linkers but also by how efficiently these different excited states transfer energy to Yb^{3+} in the inorganic SBUs to generate Yb^{3+} emission. In the case of the modified MOFs (Figure 4, blue and red curves), mixtures of different chromophores are present (Figure 3). In theory, each of these chromophores could make individual contributions to the observed excitation spectra based on its own discrete absorption profile. However, solution phase absorption spectra (Figure 4A and 4B) indicate that individual modified linkers do not absorb at wavelengths longer than 450 nm. Longer wavelength excitation (450-800 nm) observed after the modification reactions is instead attributed to higher order intermolecular π-π interactions that result from the dense packing of flexible π-systems located in MOF pores. We note that the upper limit value of absorption and excitation wavelengths observed for **MOF-1114(Yb)** and **MOF-**

1140(Yb) are similar when the MOFs are modified at the same temperature (r.t. or 75ºC) even though the overall linker conversion is significantly different between these two MOFs (Figure 3B). We contend that this observation further illustrates the importance of the confinement as fewer coupling products are required to tightly fill the smaller pores of **MOF-1140(Yb)**.

For quantification, luminescence lifetimes and quantum yields were measured at selected excitation wavelengths (Figure 4I). Unmodified **MOF-1114(Yb)** displays only one luminescence lifetime value which, consistent with its crystal structure, indicates the presence of a single type of Yb^{3+} coordination environment. **MOF-1140(Yb)** possesses two distinct luminescence lifetimes (τ_1 and τ_2) indicating the presence of two distinct coordination environments around Yb^{3+} as two of the four Yb^{3+} present in each inorganic SBU are coordinated to an additional carboxylate group (Figure 1B). τ_2 values for unmodified **MOF-1114(Yb)** and **MOF-1140(Yb)** are similar (0.644 and 0.818 μs, respectively). Based on the differences in the crystal structures discussed above, we speculate that the longer luminescence lifetime value (τ_1, 5.18 μs) observed for **MOF-1140(Yb)** specifically corresponds to the Yb^{3+} with a higher degree of coordination, decreasing the effect of quenching. Interestingly, all modified samples exhibit this additional, longer luminescence lifetime of relatively similar values (4-8 μs), although we do not attempt to explain minor trends without detailed information regarding the orientation of the newly installed pendant functional groups.

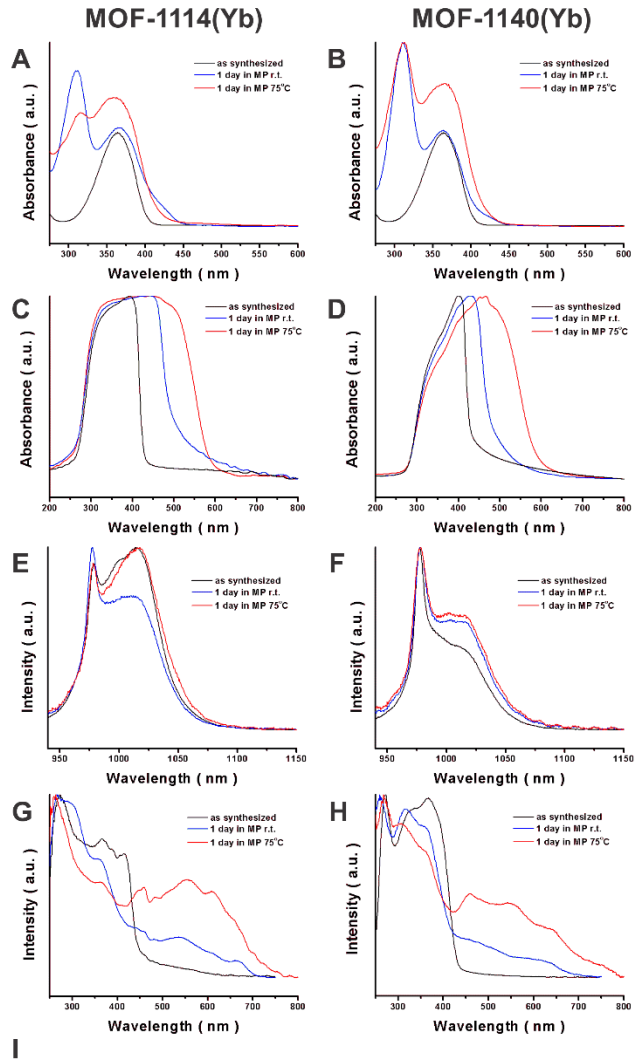

I

MOF	Sample	τ_1 / μs	τ_2 / μs	Q_{Ln} / % λ_{ex} = 380 nm	Q_{Ln} / % λ_{ex} = 600 nm
MOF-1114(Yb)	as syn.	n.a.	0.644(7)	$2.9(2)\cdot10^{-2}$	n.a.
	r.t.	4.3(2)	0.75(1)	$2.3(2)\cdot10^{-2}$	$1.87(8)\cdot10^{-2}$
	75ºC	8.2(3)	0.81(1)	$1.08(1)\cdot10^{-2}$	$1.68(8)\cdot10^{-2}$
MOF-1140(Yb)	as syn.	5.18(6)	0.818(2)	$5.5(4)\cdot10^{-2}$	n.a.
	r.t.	4.38(2)	0.79(1)	$1.5(1)\cdot10^{-2}$	$1.3(1)\cdot10^{-2}$
	75ºC	7.3(2)	0.78(1)	$1.14(2)\cdot10^{-2}$	$1.58(6)\cdot10^{-2}$

Figure 4. (A) and (B) UV-vis absorption spectra for dissolved MOFs; (C) and (D) Solid state absorption spectra for MOF crystals; (E) and (F) Yb^{3+} emission spectra under λ_{ex}=380 nm excitation; (G) and (H) Yb^{3+} excitation spectra at λ_{em}=980 nm for MOF crystals; (I) Luminescence lifetimes (τ), measured under 355 nm excitation, and quantum yields (Q_{Ln}). 2σ values are given between parentheses. Measurements taken with crystals submerged in DMF.

Quantum yields were measured under 380 and 600 nm excitation wavelengths (Figure 4I). As expected, Yb^{3+} emission in either MOF could be sensitized with 600 nm excitation wavelength only after modification. In general, quantum yields are relatively low in respect to the values reported recently for Yb^{3+} metallacrowns, for example.[26] Nevertheless, these values are comparable or higher than those reported for **Yb-PVDC-1** and **Yb-PVDC-2** that we have prepared in the past.[15] We had demonstrated that a nanoscale

version of an Yb-PVDC MOF is an attractive imaging agent for living cells and that a low quantum yield value is not a crucial

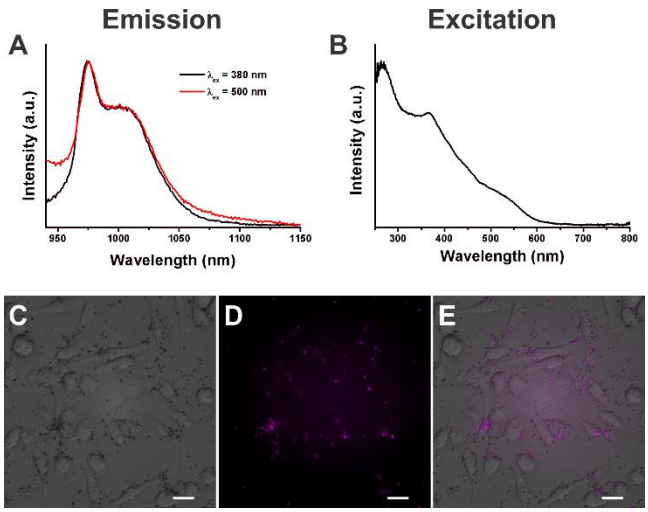

Figure 5. (A) Yb^{3+} emission spectra of miniaturized **MOF-1114(Yb)** in H_2O with 0.5% Tween-20 under λ_{ex}=380 nm and λ_{ex}=500 nm excitation; (B) Yb^{3+} excitation spectra of miniaturized MOF at λ_{em}=980 nm in H_2O with 0.5% Tween-20; (C,D,E) Microscopy images of RAW 264.7 cells incubated with miniaturized MOF in water with Tween-20 0.5 %. Objective 40x, scale bars = 20 μm: (C) Brightfield imaging; (D) NIR epifluorescence imaging; (E) Merged brightfield and NIR epifluorescence imaging.

limitation as it can be compensated for by a high density of antennae and Ln^{3+} emitters per unit volume.[20]

Epifluorescence microscopy experiments were conducted in order to test the imaging capabilities of this new family of MOFs. Images collected for **MOF-1114(Yb)** in DMF after modification with MP at 75°C (1 day) are depicted in Figure S15 and show a significant Yb^{3+} NIR emission signal. To move the demonstration further toward biological applications, intact crystals of **MOF-1114(Yb)** were broken down into smaller fragments of 2 to 3 μm through a combination of mortar and pestle grinding and ultrasonication (Figure S16). These fragments were then modified with MP at 75°C (1 day) which was found to increase their stability in water as evidenced by PXRD analysis (Figure S17). The addition of 0.5% Tween-20 prevented the aggregation of the miniaturized MOFs (Figure S18). Corresponding NIR emission and excitation spectra obtained from these particles show that they maintain their optical properties and with the observation of the characteristic Yb^{3+} NIR emission signal located at 980 nm (Figure 5A, 5B, and S19). These well dispersed and miniaturized MOFs were incubated with living RAW 264.7 macrophage cells for 18 hours. The collected NIR epifluorescence images (λ_{ex}=482 nm) showed the Yb^{3+} emission signal (Figure 5C-E, S20). These results are highly promising as they reveal that these miniaturized MOFs can sustain the biological conditions of cell culture (aqueous environment, salts, temperature) through the incubation process in the presence of living cells by continuing to generate bright emission. Such signal would have been lost had the MOFs dissociated. In addition, Figure 5C-E shows that some of the miniaturized MOFs have been concentrated on or around the macrophages. Notably, MOF fragments observed in Figure 5E are not uniformly bright which can be explained by the fact that not all organic linkers have been modified by MP during this PSM reaction (Figure 3) and the distribution of unmodified linkers throughout an intact crystal is unknown.

CONCLUSIONS

In summary our "ship-in-a-bottle" synthetic strategy produced MOFs with tightly confined chromophoric π-systems that would not otherwise be accessible and that can sensitize the NIR-emitting Yb^{3+} under biological conditions. After modification of MOFs, the resultant arrangement of pendant groups induced systemic photophysical properties; namely, broad red-shifted absorption spectra that captured most of the visible range (up to 600 nm). The absorption range was adjusted by varying the reaction temperature or MOF porosity, demonstrating the potential of this approach as a facile and efficient means of tuning the absorption/excitation wavelengths of MOFs. We have demonstrated that these chromophoric π-systems are suitable as novel, small-sized and versatile antennae for the sensitization of the NIR emission of Yb^{3+}. Although the quantum yields recorded for Yb^{3+} emission are relatively low, this MOF design approach allows for a high density of luminescent Ln^{3+} and Ln^{3+}-sensitizers per unit volume and for the facile tuning of chromophores in order to achieve better protection of Ln^{3+} from quenching by saturating their coordination sphere or enhancing sensitization efficiency. In general, reactions promoted within predefined nanoscale cavities can produce π-conjugated groups from smaller discrete molecular building blocks. Because the cavity has predefined and constant dimensions, the strength and number of intermolecular π-π interactions increases with the yield and average size of the π-conjugated systems and can be modulated by controlling factors such as reaction time and temperature. Further, this increase in the density of π-conjugated systems has a dominant influence on the spectroscopic properties of the material. Preliminary optical microscopy tests show that these bulk Yb^{3+} MOFs and their corresponding miniaturized fragments are promising NIR optical imaging agents. We have shown that these materials are sufficiently robust and bright to collect a significant NIR signal in typical biological conditions used for living cell incubation and imaging.

ASSOCIATED CONTENT

Supporting Information

The Supporting Information is available free of charge on the ACS Publications website.

Experimental details and additional data (PDF)

Crystallographic data for **MOF-1140(Yb)** CCDC 1886235 (CIF)

AUTHOR INFORMATION

Corresponding Author

*nrosi@pitt.edu

*stephane.petoud@inserm.fr

Notes

The authors declare no competing financial interests.

ACKNOWLEDGMENT

P.F.M. received partial support from Oak Ridge Institute for Science and Education (ORISE) professional internship program at the National Energy Technology Laboratory (NETL). S.P. acknowledges support from Institut National de la Santé et de la Recherche Médicale (INSERM). In addition, this work is partially supported by la Ligue Contre le Cancer, La Région Centre, Agence Nationale de la Recherche (NIRA ANR-13-BS08-0011) and the Réseau Canaux Ioniques du Cancéropôle Grand Ouest. Results incorporated in the standard have received funding from the European Union's Horizon 2020 Research and Innovation Program under the Marie Sklodowska-Curies Grant agreement No 665790. The authors also thank the University of Pittsburgh and the Petersen Nano Fabrication and Characterization Facility at the University of Pittsburgh for access to PXRD and microspectrophotometry instrumentation.

REFERENCES

1. Eliseeva, S. V.; Bünzli, J.-C. G., Lanthanide luminescence for functional materials and bio-sciences. *Chem. Soc. Rev.* **2010,** *39*, 189-227.

2. Bünzli, J.-C. G.; Eliseeva, S. V., Intriguing aspects of lanthanide luminescence. *Chem. Sci.* **2013,** *4*, 1939-1949.

3. Martinić, I.; Eliseeva, S. V.; Petoud, S., Near-infrared emitting probes for biological imaging: Organic fluorophores, quantum dots, fluorescent proteins, lanthanide(III) complexes and nanomaterials. *J. Lumin.* **2016,** *189*, 19-43.

4. Beeby, A.; M. Clarkson, I.; S. Dickins, R.; Faulkner, S.; Parker, D.; Royle, L.; S. de Sousa, A.; A. Gareth Williams, J.; Woods, M., Non-radiative deactivation of the excited states of europium, terbium and ytterbium complexes by proximate energy-matched OH, NH and CH oscillators: an improved luminescence method for establishing solution hydration states. *J. Chem. Soc., Perkin Trans. 2* **1999,** *0*, 493-504.

5. Doffek, C.; Alzakhem, N.; Molon, M.; Seitz, M., Rigid, Perdeuterated Lanthanoid Cryptates: Extraordinarily Bright Near-IR Luminophores. *J. Am. Chem. Soc.***2010,** *132*, 14334-14335.

6. Uh, H.; Petoud, S., Novel antennae for the sensitization of near infrared luminescent lanthanide cations. *Inorg. Chem.* **2010,** *13*, 668-680.

7. Weissman, S. I., Intramolecular Energy Transfer The Fluorescence of Complexes of Europium. *J. Chem. Phys.* **1942,** *10*, 214-217.

8. Bauer, C. A.; Bhakta, R. K.; Houk, R. J. T.; Allendorf, M. D., Luminescent Metal–Organic Frameworks *Chem. Soc. Rev.* **2009,** *38*, 1330-1352.

9. Cui, Y.; Chen, B.; Qian, G., Lanthanide metal-organic frameworks for luminescent sensing and light-emitting applications. *Coord. Chem. Rev.* **2014,** *273*, 76-86.

10. Ma, L.; Evans, O. R.; Foxman, B. M.; Lin, W., Luminescent Lanthanide Coordination Polymers. *Inorg. Chem.,* **1999,** *38,* 5837–5840.

11. Reineke, T. M.; Eddaoudi, M.; Feher, M.; Kelley, D.; Yaghi, O. M., From Condensed Lanthanide Coordination Solids to Microporous Frameworks Having Accessible Metal Sites. *J. Am. Chem. Soc.,* **1999***, 121,* 1651–1657.

12. de Lill, D. T.; de Bettencourt-Dias, A.; Cahill, C. L., Exploring Lanthanide Luminescence in Metal-Organic Frameworks: Synthesis, Structure, and Guest-Sensitized Luminescence of a Mixed Europium/Terbium-Adipate Framework and a Terbium-Adipate Framework. *Inorg. Chem.*, **2007**, *46* , 3960 -3965.

13. Cui, Y.; Song, R.; Yu, J.; Liu, M.; Wang, Z.; Wu, C.; Yang, Y.; Wang, Z.; Chen, B.; Qian, G., Dual-Emitting MOF⊃Dye Composite for Ratiometric Temperature Sensing. *Adv. Mater.* **2015,** *27*, 1420-1425.

14. Lian, X.; Yan, B., A lanthanide metal–organic framework (MOF-76) for adsorbing dyes and fluorescence detecting aromatic pollutants. *RSC Adv.*, **2016**, *6* , 11570 -11576.

15. White, K. A.; Chengelis, D. A.; Zeller, M.; Geib, S. J.; Szakos, J.; Petoud, S.; Rosi, N. L., Near-infrared emitting ytterbium metal-organic frameworks with tunable excitation properties. *Chem. Comm.* **2009,** *0*, 4506-4508.

16. White, K. A.; Chengelis, D. A.; Gogick, K. A.; Stehman, J.; Rosi, N. L.; Petoud, S., Near-Infrared Luminescent Lanthanide MOF Barcodes. *J. Am. Chem. Soc.* **2009,** *131*, 18069-18071.

17. An, J.; Shade, C. M.; Chengelis-Czegan,, D. A.; Petoud, S.; Rosi, N. L., Zinc-adeninate metal-organic framework for aqueous encapsulation and sensitization of near-infrared and visible emitting lanthanide cations. *J. Am. Chem. Soc.* **2011,** *133*, 1220-1223.

18. Luo, T.-Y.; Liu, C.; Eliseeva, S. V.; Muldoon, P. F.; Petoud, S.; Rosi, N. L., Rare Earth pcu Metal–Organic Framework Platform Based on RE4(μ3-OH)4(COO)62+ Clusters: Rational Design, Directed Synthesis, and Deliberate Tuning of Excitation Wavelengths. *J. Am. Chem. Soc.* **2017,** *139*, 9333-9340.

19. Liu, C.; Eliseeva, S. V.; Luo, T.-Y.; Muldoon, P. F.; Petoud, S.; Rosi, N. L., Near infrared excitation and emission in rare earth MOFs via encapsulation of organic dyes. *Chem. Sci.* **2018**, *9*, 8099-8102.

20. Foucault-Collet, A.; Gogick, K. A.; White, K. A.; Villette, S.; Pallier, A.; Collet, G.; Kieda, C.; Li, T.; Geib, S. J.; Rosi, N. L.; Petoud, S., Lanthanide near infrared imaging in living cells with Yb3+ nano metal organic frameworks. *Proc. Natl. Acad. Sci. U.S.A.* **2013,** *110*, 17199-17204.

21. Cohen, S. M., Postsynthetic Methods for the Functionalization of Metal–Organic Frameworks. *Chem. Rev.* **2012,** *112*, 970-1000.

22. Bottomley, W., The reaction of amines with methyl propiolate. *Tetrahedron Lett.* **1967,** *8*, 1997-1999.

23. Ji, M.; Lan, X.; Han, Z.; Hao, C.; Qiu, J., Luminescent Properties of Metal–Organic Framework MOF-5: Relativistic Time-Dependent Density Functional Theory Investigations. *Inorg. Chem.* **2012,** *51*, 12389-12394.

24. Dolgopolova, E. A.; Rice, A. M.; Smith, M. D.; Shustova, N. B., Photophysics, Dynamics, and Energy Transfer in Rigid Mimics of GFP-based Systems. *Inorg. Chem.* **2016,** *55*, 7257-7264.

25. Gonçalves e Silva, F. R.; Malta, O. L.; Reinhard, C.; Güdel, H.-U.; Piguet, C.; Moser, J. E.; Bünzli, J.-C. G., Visible and Near-Infrared Luminescence of Lanthanide-Containing Dimetallic Triple-Stranded Helicates: Energy Transfer Mechanisms in the SmIII and YbIII Molecular Edifices. *J. Phys. Chem. A* **2002,** *106*, 1670-1677.

26. Chow, C. Y.; Eliseeva, S. V.; Trivedi, E. R.; Nguyen, T. N.; Kampf, J. W.; Petoud, S.; Pecoraro, V. L., Ga3+/Ln3+ Metallacrowns: A Promising Family of Highly Luminescent Lanthanide Complexes That Covers Visible and Near-Infrared Domains. *J. Am. Chem. Soc.* **2016,** *138*, 5100-5109.

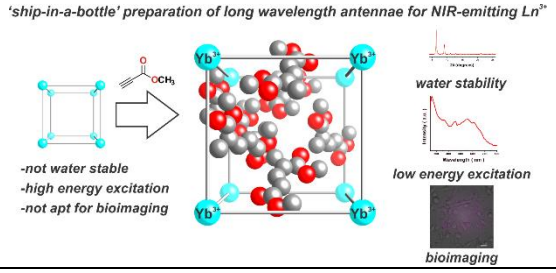
'ship-in-a-bottle' preparation of long wavelength antennae for NIR-emitting Ln^{3+}
Yb^{3+}
Yb^{3+}
Yb^{3+}
Yb^{3+}
OCH_3
-not water stable
-high energy excitation
-not apt for bioimaging
water stability
low energy excitation
bioimaging